ABNORMAL POLLEN TUBE GUIDANCE1, an Endoplasmic Reticulum-Localized Mannosyltransferase Homolog of GLYCOSYLPHOSPHATIDYLINOSITOL10 in Yeast and PHOSPHATIDYLINOSITOL GLYCAN ANCHOR BIOSYNTHESIS B in Human, Is Required for Arabidopsis Pollen Tube Micropylar Guidance and Embryo Development[1][W][OPEN]

Xin Ren Dai[2], Xin-Qi Gao[2], Guang Hui Chen, Li Li Tang, Hao Wang, and Xian Sheng Zhang*

State Key Laboratory of Crop Biology, Shandong Key Laboratory of Crop Biology, College of Life Sciences, Shandong Agricultural University, Taian 271018, China

ORCID ID: 0000-0002-3129-5206 (X.S.Z.).

The perception and response of pollen tubes to the female guidance signals are crucial for directional pollen tube growth inside female tissues, which leads to successful reproduction. In pursuing the mechanisms underlying this biological process, we identified the Arabidopsis (*Arabidopsis thaliana*) *abnormal pollen tube guidance1* (*aptg1*) mutant, whose pollen tubes showed compromised micropylar guidance. In addition to its male defect, the *aptg1* mutant showed embryo lethality. *APTG1* encodes a putative mannosyltransferase homolog to human PHOSPHATIDYLINOSITOL GLYCAN ANCHOR BIOSYNTHESIS B and yeast (*Saccharomyces cerevisiae*) GLYCOSYLPHOSPHATIDYLINOSITOL10 (GPI10), both of which are involved in the biosynthesis of GPI anchors. We found that *APTG1* was expressed in most plant tissues, including mature pollen, pollen tubes, mature embryo sacs, and developing embryos. By fluorescence colabeling, we showed that APTG1 was localized in the endoplasmic reticulum, where GPI anchors are synthesized. Disruption of *APTG1* affected the localization of COBRA-LIKE10, a GPI-anchored protein important for pollen tube growth and guidance. The results shown here demonstrate that APTG1 is involved in both vegetative and reproductive development in Arabidopsis, likely through processing and proper targeting of GPI-anchored proteins.

Double fertilization is the biological basis for seed propagation and plant reproduction in angiosperms. Pollen tubes grow through maternal tissue to deliver the immobile sperm cells into the female gametophyte (embryo sac). During this process, pollen tube guidance into the micropyle is a critical step and is precisely regulated (Dresselhaus and Franklin-Tong, 2013). Female guidance signals are generated by both sporophytic and gametophytic tissues and operate at different stages during pollen tube growth. The sporophytic signal directs the growth of pollen tubes in the stigma, style, and transmitting tract. The signal that induces pollen tubes to turn to the funiculus and grow into the micropyle is termed gametophytic guidance (Shimizu and Okada, 2000; Higashiyama et al., 2003). Extensive cellular and genetic studies have demonstrated that female gametophytes play key roles in the micropylar guidance of pollen tubes (Kasahara et al., 2005; Márton et al., 2005; Chen et al., 2007; Alandete-Saez et al., 2008; Okuda et al., 2009; Kessler and Grossniklaus, 2011; Takeuchi and Higashiyama, 2011). The molecular natures of such guidance signals have been gradually revealed in recent years (i.e. small peptides secreted by the female gametophyte, egg apparatus, or synergid cells; Márton et al., 2005; Jones-Rhoades et al., 2007; Okuda et al., 2009).

Pollen tubes need to perceive the female guidance signals at the cell surface to initiate intracellular responses for directional growth. However, the mechanisms of pollen tube perception are still obscure. A few male factors involved in signal perception during pollen tube growth into ovules have been identified. For example, the Arabidopsis (*Arabidopsis thaliana*) sperm cell-specific protein HAPLESS2/GENERATIVE CELL-SPECIFIC1 was necessary for pollen tubes to target the micropyle (von Besser et al., 2006). Arabidopsis

[1] This work was supported by the Major Research Plan from the Ministry of Science and Technology of China (grant no. 2013CB945100) and the National Natural Science Foundation of China (grant nos. 31170293 and 31270358).

[2] These authors contributed equally to the article.

* Address correspondence to zhangxs@sdau.edu.cn.

The author responsible for distribution of materials integral to the findings presented in this article in accordance with the policy described in the Instructions for Authors (www.plantphysiol.org) is: Xian Sheng Zhang (zhangxs@sdau.edu.cn).

[W] The online version of this article contains Web-only data.

[OPEN] Articles can be viewed online without a subscription.

www.plantphysiol.org/cgi/doi/10.1104/pp.114.236133

CATION/PROTON EXCHANGER21 (*CHX21*) and *CHX23* encode K^+ transporters in growing pollen tubes. Pollen grains of the *chx21 chx23* double mutant germinated and extended a normal tube in the transmitting tract, but their targeting of the funiculus failed (Lu et al., 2011). Arabidopsis *POLLEN DEFECTIVE IN GUIDANCE1* (*POD1*) was expressed in pollen grains, pollen tubes, and synergid cells. The *pod1* pollen tubes showed defective micropylar guidance (Li et al., 2011). The tip of the pollen tube has been hypothesized to be the site of cue perception for micropyle-directed growth. The Arabidopsis Rab GTPase RABA4D was localized at the tips of growing pollen tubes. Pollen tubes with defective RABA4D had severely reduced growth rates and ovule targeting (Szumlanski and Nielsen, 2009). Recently, two receptor-like kinases at the apical plasma membrane (PM) of growing pollen tubes, LOST IN POLLEN TUBE GUIDANCE1 (LIP1) and LIP2, were demonstrated to guide pollen tubes to the micropyle by perceiving the AtLURE1 signal from synergid cells (Liu et al., 2013).

Glycosylphosphatidylinositol (GPI) anchoring provides a strategy for targeting proteins to the outer layer of the PMs in eukaryotic cells. GPI anchors are synthesized inside the endoplasmic reticulum (ER) and are attached to proteins by posttranslational modifications in the ER. After processing, GPI-anchored proteins (GPI-APs) are transported to the cell surface following an unknown trafficking route and anchored at the cell surface (Maeda and Kinoshita, 2011). GPI-APs play very important roles in plant reproductive development (Gillmor et al., 2005; Ching et al., 2006; DeBono et al., 2009). An Arabidopsis putative GPI-AP, LORELEI, functioned in pollen tube reception of female signals, double fertilization, and early seed development (Capron et al., 2008; Tsukamoto et al., 2010). Arabidopsis COBRA-LIKE10 (COBL10), a GPI-AP, regulates the polar deposition of wall components in pollen tubes growing inside female tissues and is critical for micropylar guidance (Li et al., 2013). The conserved backbone of GPI anchors in eukaryotes is ethanolamine phosphate-6-Man-α-1,2-Man-α-1,6-Man-α-1,4-glucosamine-α-1,6-myoinositol phospholipid. During the biosynthesis of GPI anchors, monosaccharides, fatty acids, and phosphoethanolamines are sequentially added onto phosphatidylinositol. This process involves at least 16 enzymes and cofactors in mammals, including PHOSPHATIDYLINOSITOL GLYCAN ANCHOR BIOSYNTHESIS (PIG) A, B, C, F, G, H, L, M, N, O, P, Q, V, W, X, and Y (Maeda and Kinoshita, 2011). The core structure of the GPI anchor contains three Man residues donated by the substrate dolichol-phosphate-Man. GPI mannosyltransferases were required for adding the three Man residues of the GPI anchor in the ER lumen (Maeda and Kinoshita, 2011). Arabidopsis PEANUT1 (PNT1) is a homolog of the mammalian GPI mannosyltransferase PIG-M, involved in the addition of the first Man during the biosynthesis of the GPI anchor. The *pnt1* mutant showed the defect of pollen viability and embryo development (Gillmor et al., 2005). *PIG-B* of human and *GPI10* of yeast (*Saccharomyces cerevisiae*) encode GLYCOSYLPHOSPHATIDYLINOSITOL MANNOSYLTRANSFERASE3, involved in the addition of the third Man during the biosynthesis of the GPI anchor (Takahashi et al., 1996; Sütterlin et al., 1998). Mutation of *PIG-B* and *GPI10* resulted in the accumulation of the GPI intermediate Man2-glucosamine-(acyl) phosphatidylinositol and led to cell death in yeast.

In this study, we identified the ER-localized ABNORMAL POLLEN TUBE GUIDANCE1 (APTG1), an Arabidopsis homolog of PIG-B and GPI10. Pollen tubes of the *aptg1* mutant showed compromised directional growth to the micropyle and lost the apical PM localization of COBL10. Besides the male defect, the mutant showed embryo lethality. In addition, reducing the expression of *APTG1* resulted in defective seedling growth, indicating that APTG1 plays important roles in both reproductive and vegetative development.

RESULTS

aptg1 Showed Reduced Male Transmission

To understand the mechanism of pollen tube guidance, we tried to isolate Arabidopsis transfer DNA (T-DNA) insertion mutants showing abnormal pollen tube guidance from the Arabidopsis T-DNA insertion collection of the Arabidopsis Biological Resource Center. A pollen tube guidance mutant (SALK_080854) was identified, and it was named *aptg1*. In this mutant, the T-DNA was inserted in the fifth intron of the genomic sequence of AT5G14850 (1,930 bp downstream from the initiation codon ATG). The progeny genotypes of the heterozygous plants (*aptg1*/+) were identified by a PCR-based method using gene-specific primers and the T-DNA primer (Fig. 1A). However, we did not find homozygous plants in these offspring (Table I). Next, we analyzed the phenotypes of heterozygous plants and did not observe any difference from the wild-type plants. For example, the seed number and the length of a silique of heterozygous plants are nearly equal to those of the wild type (Supplemental Fig. S1). The genotype ratio between the wild-type and heterozygous plants of the offspring from the heterozygous plant was about 1:0.9 (207:185; Table I), implying that the *aptg1* gametophyte was defective. To dissect which gametophyte was defective, we made reciprocal crosses between the wild-type plant and the heterozygous mutant and examined the genotypes of the progeny. We found that 96.9% of the mutant allele was transmitted via the female gametophytes, while only 8.3% of transmission occurred via the male gametophytes (Table I). This result implies that APTG1 is necessary for male gametophyte function.

Pollen Germination and Tube Growth Are Not Affected by the Mutation at *APTG1*

To dissect whether the dysfunctional male gametophyte of the *aptg1*/+ mutant was due to defective pollen, we examined the viability, nuclei, and morphology

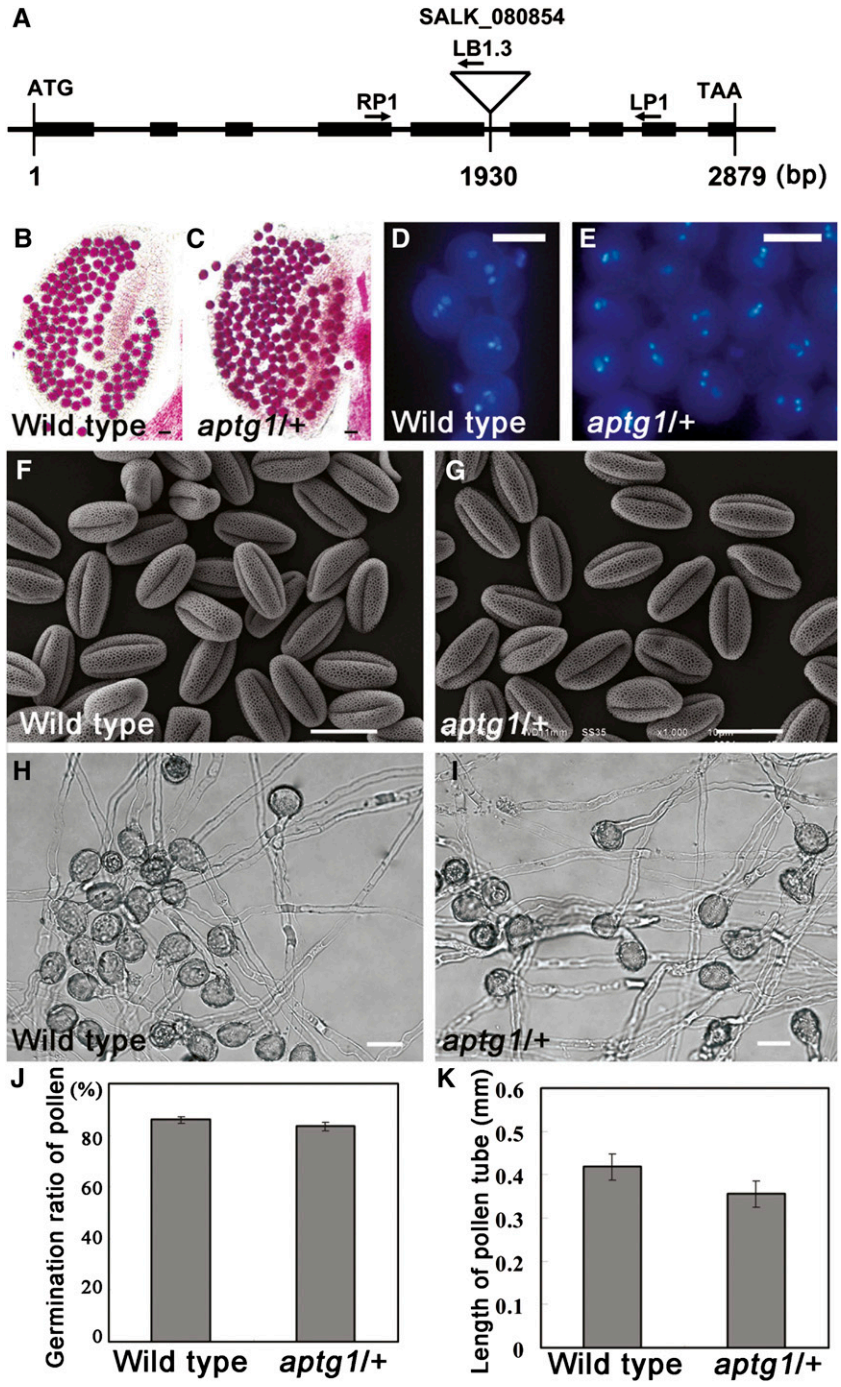

Figure 1. Pollen viability, germination, and tube growth of the heterozygous *aptg1*/+ mutant and wild-type pollen. A, Schematic representation of *APTG1* genomic organization and the T-DNA position in SALK_080854. Exons of *APTG1* are represented by black boxes and introns by lines. The location of the T-DNA insertion of SALK_080854 is indicated with the triangle. Primer LB1.3 is for the left border of the T-DNA, and RP1 and LP1 are gene-specific primers at upstream and downstream locations, respectively. B to E, Mature pollen grains of the wild type (B and D) and *aptg1*/+ (C and E) with Alexander (B and C) and DAPI (D and E) staining. F and G, Mature pollen grains of the wild type (F) and *aptg1*/+ (G) observed by SEM. H and I, Wild-type (H) and *aptg1*/+ (I) pollen germination in vitro. J and K, Pollen germination ratio and pollen tube length in vitro for 4 h, showing no significant differences between the wild type and the *aptg1*/+ mutant (Student's *t* test, $P > 0.05$). Bars = 20 μm.

of mature pollen grains by Alexander staining, 4,6-diamidino-2-phenylindole (DAPI) staining, and scanning electron microscopy (SEM), respectively. No difference in viability or morphology was detected between the *aptg1*/+ mutant and the wild-type mature pollen grains (Fig. 1, B, C, F, and G). Most pollen grains contained two generative nuclei and one vegetative nucleus in both the wild type and the *aptg1*/+ mutant (Fig. 1, D and E). Then, we examined the germination and tube growth of pollen in vitro to determine why the mutant allele was not transmitted via the male gametophyte. We found that the pollen germination ratio and pollen tube morphology of the *aptg1*/+ mutant were comparable with those of the wild type in vitro (Fig. 1, H–J). Furthermore, we measured the lengths of pollen tubes germinated in vitro for 4 h but did not find any significant difference between the *aptg1*/+ mutant and the wild type (Fig. 1K), indicating that the *APTG1* mutation does not result in abnormal pollen germination or pollen tube growth in vitro.

Table I. *Segregation of selfed and crossed progeny of the aptg1/+ mutant and the genetic transmission of the aptg1 allele*

ND, Not determined.

Progeny	Genotype[a]					
	APTG1/+	*aptg1/+*	*aptg1/−*	Ratio	Expected Ratio	Transmission Efficiency[b]
Self-pollination						
♀ *aptg1/+* × ♂ *aptg1/+*	207	185	0	1:0.89:0	1:2:1	ND
Reciprocal pollination						
♀ *aptg1/+* × ♂ Wild type	96	93	0	1:0.97:0	1:1:0	96.9%
♀ Wild type × ♂ *aptg1/+*	109	9	0	1:0.08:0	1:1:0	8.3%[c]
Limited pollination[d]						
♀ Wild type × ♂ *aptg1/+*	88	28	0	1:0.32:0	1:1:0	31.8%[c]

[a]The genotypes of progeny were analyzed by a PCR-based method as described in "Materials and Methods." [b]The genetic transmission of *aptg1* was calculated according to Howden et al. (1998). The transmission efficiency equals *aptg1/+*/*APTG1/+* × 100%. [c]There are significant differences of transmission efficiency between them (Student's *t* test, $P < 0.01$). [d]The number of pollen grains pollinated on one stigma is less than 40.

Pollen Tubes of *aptg1* Were Compromised in Micropylar Guidance

To investigate the defective transmission of *aptg1* through male gametophytes, we calculated the transmission efficiency of the *aptg1* allele by applying a limited amount (less than 40 grains) of heterozygous *aptg1/+* mutant pollen to the emasculated wild-type pistil. We found that the transmission efficiency (31.8%) with limited pollination was much higher than with excessive pollen grains, but it was still less than the expected 100% (Table I), indicating that pollen with the mutant *aptg1* allele had a competitive disadvantage compared with the wild type for fertilization. To further dissect why the mutant pollen was less competitive, we observed the growth of pollen tubes in pistils at 24 h after limited pollination using Aniline Blue staining and SEM. When *aptg1/+* pollen was used, no abnormalities were observed during pollen tube growth in the style or transmitting tract (Supplemental Fig. S2). Then, we observed pollen tube micropylar guidance. We found that about 52.3% (n = 512) of pollen tubes grew normally and entered the micropyle (Fig. 2, A and F), but many pollen tubes showed abnormal guidance near the micropyle. These pollen tubes showing abnormal guidance can be further broken down into two categories: growth on the surfaces of the ovules or the funiculus but missing the micropyle (nontargeting; 27.4% of pollen tubes [n = 512]; Fig. 2, B, C, and F) and twisted growth around the micropyles before finally entering them (targeting; 20.3% of pollen tubes [n = 512]; Fig. 2, D and F). Additionally, two pollen tubes targeting one ovule were observed, but only one tube could enter the micropyle (Fig. 2E). Similar abnormal guidance of the *aptg1/+* pollen tube was observed by SEM (Supplemental Fig. S3, A–D). These abnormal growth patterns might result from the *aptg1* mutation, because theoretically, about 50% of pollen grains harbor the *aptg1* allele in the *aptg1/+* heterozygote. In contrast, abnormal growth of pollen tubes around the micropyle was rarely observed (0.3%; n = 450) when wild-type pollen was used for limited pollination. These results suggest that the micropylar response of the *aptg1* pollen tube is compromised.

To confirm the function of *APTG1*, we amplified the predicted promoter (1,799 bp) and coding sequence (CDS) of *APTG1*, subcloned them into pCAMBIA1300 vector (conferring hygromycin resistance to transgenic plants), and introduced them into the *aptg1/+* heterozygote through *Agrobacterium tumefaciens*-mediated infiltration. The T-DNA sequence in the *aptg1/+* mutant contains a kanamycin resistance gene (Kan^r). We found that the Kan^r:Kan^s (for kanamycin susceptible) ratio of the offspring from *aptg1/+* heterozygous plant was nearly 1:1, and the Kan^r plants were all *aptg1/+* mutants identified by the PCR-based method. Thirty independent transformants with the *aptg1/+* background were obtained using kanamycin and hygromycin selection and named *aptg1/+* $APTG1_{CDS}$ (T1 generation). Then, we performed kanamycin resistance segregation analysis by plating the selfed progeny seeds (T2 generation) of several randomly selected lines, as described by Li et al. (2011). The Kan^r:Kan^s ratio rose to 1.8:1 to 2.67:1 in the *aptg1/+* $APTG1_{CDS}$ transgenic plants, and it was much higher than in the *aptg1/+* mutant plants (Table II). Furthermore, the proportion of normal pollen tube guidance was significantly increased in the *aptg1/+* $APTG1_{CDS}$ transgenic line compared with abnormal guidance (Supplemental Fig. S4). These results showed that the CDS of *APTG1* could recover defects in pollen tube guidance in the *aptg1/+* mutant. Additionally, we inhibited the expression of *APTG1* in pollen tubes by an artificial microRNA (amiRNA) technology according to Schwab et al. (2006). Fourteen transgenic lines expressing Late anther tomato gene52 (Lat52)::*amiRNA-APTG1* were obtained, and the pollen tube guidance in T2 generation transgenic plants was examined following the limited pollination transgenic pollen onto the wild-type emasculated pistils. Most of the pollen tubes showed misguidance for the micropyle under limited pollination (Supplemental Fig. S5). Therefore, the pollen tube misguidance in our study might be involved in the *aptg1* mutation.

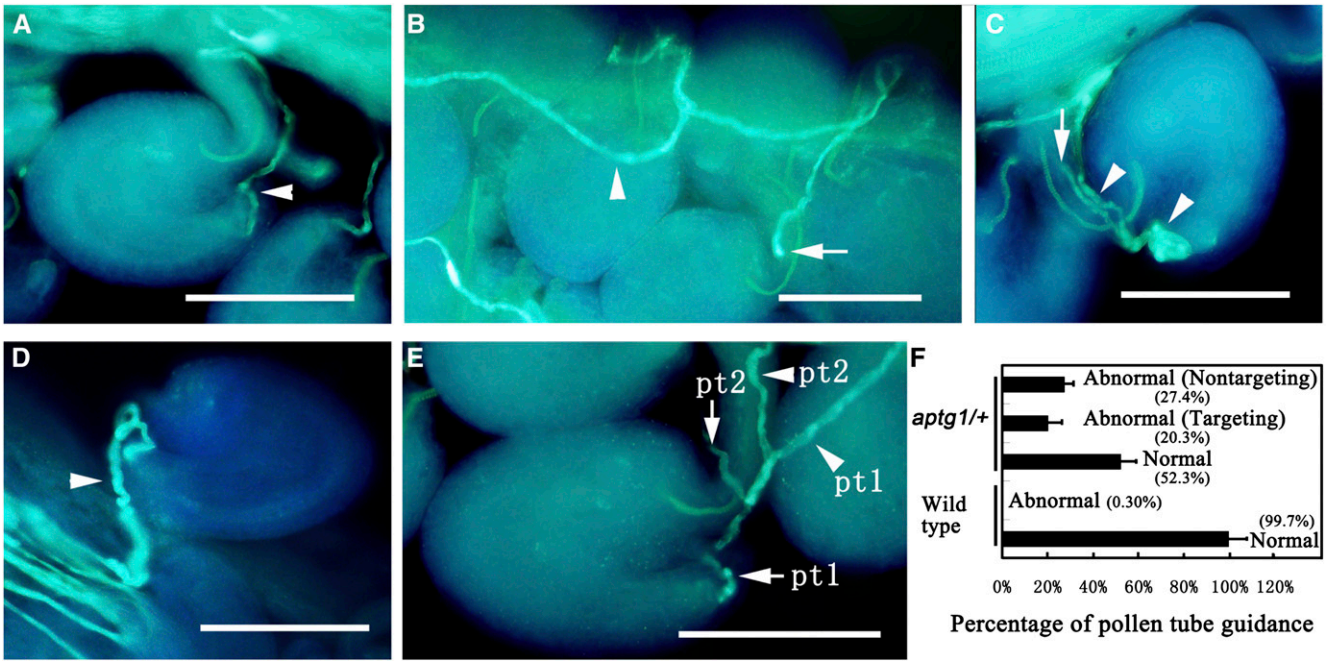

Figure 2. Guidance of the heterozygous *aptg1/+* and wild-type pollen tubes analyzed with Aniline Blue staining. Emasculated wild-type pistils were pollinated with limited amounts of wild-type pollen (A) or *aptg1/+* pollen (B–E) and observed 24 h after pollination. A, Wild-type normal pollen tube guidance. B, *aptg1/+* pollen tube winding among ovules without entering a micropyle. C, *aptg1/+* pollen tube twisting around the micropyle but without entering it. D, *aptg1/+* pollen tube twisting around the micropyle but eventually entering it. E, Two *aptg1/+* pollen tubes grow toward the micropyle. One pollen tube (pt1) enters the micropyle, but the other (pt2) fails to reach the micropyle. F, Percentage of normal and abnormal guidance of pollen tubes in the wild type and the *aptg1/+* mutant. The pollen tubes showing abnormal guidance in *aptg1/+* include two types: growth on the surfaces of the ovules but missing the micropyle (nontargeting) and twisted growth around the micropyles before finally entering them (targeting). The numbers at the ends of the black bars indicate the percentages of different types of pollen tubes. Statistical analysis of pollen tube guidance revealed that there were no differences between normal and abnormal guidance in the *aptg1/+* mutant (Student's *t* test, $P > 0.05$). Data were collected from three independent experiments. Arrowheads indicate the pollen tubes, and arrows indicate the growing apices of pollen tubes. Bars = 100 μm.

Functional Loss of *APTG1* Affected Early Embryo Development

Our analysis demonstrated that about 20.3% of pollen tubes showed abnormal guidance but still entered the micropyle, and the transmission efficiency of the *aptg1* allele through male gametophytes increased with limited pollination (Table I). However, we did not obtain any homozygous *aptg1* mutants from the selfed progeny of the *aptg1/+* plants. This suggested that development of the *aptg1/−* embryo is defective. To test this hypothesis, we observed embryo development in *aptg1/+* ovaries at 3 and 4 d after limited pollination with *aptg1/+* pollen. We found that most of the early embryos (88.8%) reached the globular and heart-shaped embryo stages at 3 and 4 d after pollination (Fig. 3, A and G). The development of about 11.2% of embryos was retarded at the globular embryo or earlier stages (Fig. 3, B–E and H–J), which was about half of the percentage (20.3%) of pollen tubes showing twisted growth around the micropyle, but entered the micropyle finally under limited pollination conditions. It was suggested that these retarded developmental embryos were the homozygotes of *aptg1*. Furthermore, we observed that cell division was retarded after the first division of zygotes in some abnormal embryos (Fig. 3, B, C, and H). In other abnormal embryos, cell division in the embryo proper was inhibited (Fig. 3D) or the suspensor cell showed lateral overexpansion (Fig. 3E). The transverse multiple divisions and abnormal oblique division of embryo-proper cells were also observed in the homozygotic embryo of the

Table II. *Segregation analysis of the selfed progeny of aptg1/+ mutant and aptg1/+ $APTG1_{CDS}$ lines*

Progeny	Kan^r	Kan^s	Kan^r/ Kan^s
aptg1/+	206	207	0.995:1[a]
aptg1/+ $APTG1_{CDS}$ line 6	124	61	2.03:1
aptg1/+ $APTG1_{CDS}$ line 9	131	57	2.30:1
aptg1/+ $APTG1_{CDS}$ line 17	251	139	1.81:1
aptg1/+ $APTG1_{CDS}$ line 18	147	55	2.67:1
aptg1/+ $APTG1_{CDS}$ line 26	169	92	1.84:1

[a]The Kan^r:Kan^s ratio of the selfed progeny of the *aptg1/+* mutant was nearly 1:1, and the genotype of Kan^r plants was all *aptg1/+* identified by a PCR-based method.

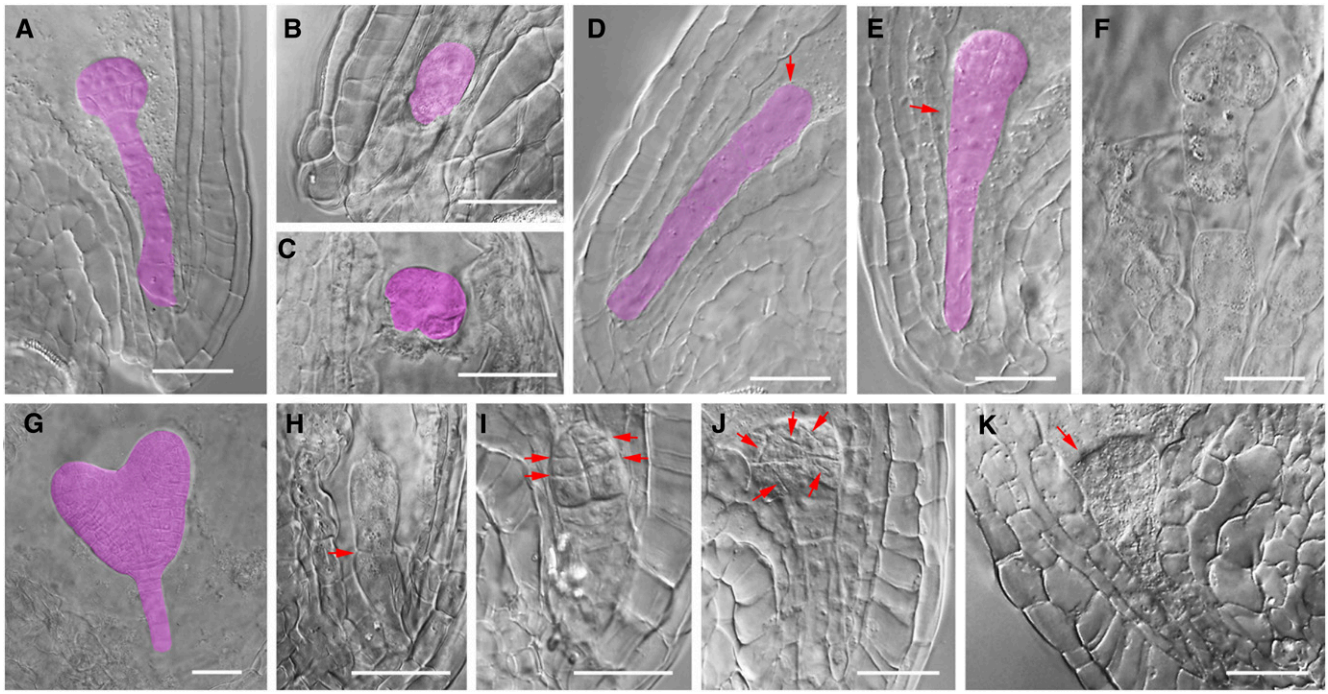

Figure 3. Early embryo development in the *aptg1*/+ pistil. A to F, Embryo development 3 d after limited pollination using *aptg1*/+ pollen and emasculated *aptg1*/+ pistils. A, Globular embryo showing normal development. B to F, Putative homozygous mutant embryos showing abnormal development at different stages, including retarded development at the two-cell stage (B), amorphous zygotic tissue (C), retarded apical cell division (arrow; D), abnormal suspensor cell (arrow) at the globular stage (E), and a degenerating globular embryo (F). G to K, Embryo development 4 d after limited pollination using *aptg1*/+ pollen and emasculated *aptg1*/+ pistils. G, Heart-shaped embryo showing normal development. H to K, Putative homozygous mutant embryos showing abnormal development at different stages, including a retarded and degenerating two-cell embryo (arrow; H), abnormal transverse division (arrows) of the apical cell (I), abnormal oblique division (arrows) of the apical cell (J), and a degenerating globular embryo (arrow; K). Pseudocolor was used to depict the young embryos in A to E and G. Bars = 20 μm.

aptg1 mutant (Fig. 3, I and J). These retarded embryos started degenerating at the globular embryo stage (Fig. 3, F and K). In contrast, in the wild-type siliques pollinated with limited *aptg1*/+ pollen, the development of embryo reached the globular and heart-shaped embryo stages at 3 and 4 d after pollination, and no (n = 189) abnormal developing embryo was observed. The difference of the embryo defect percentage between the *aptg1*/+ and the wild-type siliques is statistically significant (Student's t test, $P < 0.01$). These results imply that APTG1 is important for the vegetative development of Arabidopsis. To confirm this hypothesis, we made an amiRNA construct (35S::*amiRNA-APTG1*) and transformed it into Arabidopsis to decrease the expression level of *APTG1*. The transgenic seedling growth was inhibited markedly, indicating that APTG1 is required for seedling growth (Supplemental Fig. S6).

APTG1 Encodes a Mannosyltransferase

APTG1 encodes a putative protein of 548 amino acids that belongs to the Alg9-like mannosyltransferase family. Some members of this family are localized in the ER and are involved in GPI anchor biosynthesis. The mannosyltransferase domain of APTG1 contains eight transmembrane helices, indicating that APTG1 is a membrane-anchored protein (Fig. 4A). Phylogenetic analysis indicated that APTG1 shared high homology with several proteins from dicotyledons, such as *Arabidopsis lyrata*, *Vitis vinifera*, *Ricinus communis*, *Medicago truncatula*, and *Glycine max* (Fig. 4B). The HKEXRF motif is a conserved signature sequence for mannosyltransferase PIG-B homologs of various species (Oriol et al., 2002). Protein sequence alignments revealed an HKEFRF motif near the C terminus of APTG1 (Fig. 4C). APTG1 shares 24.8% and 34.9% identities with the yeast GPI10 and human PIG-B proteins, respectively (Fig. 4D), and both mannosyltransferases are involved in the addition of the third Man of the GPI anchor (Takahashi et al., 1996; Sütterlin et al., 1998). To determine whether APTG1 can functionally substitute for the yeast GPI10, the full-length CDS of *APTG1* was cloned behind the pGAL1 promoter and transformed into a yeast *gpi10* mutant YGL142c thermosensitive strain that could not grow at 37°C. The transfected yeast clone expressing the CDS of *APTG1* eliminated the thermosensitivity of the *gpi10* mutant. In contrast, the empty vector could not complement the phenotype of the *gpi10* mutant. Thus, APTG1 might be a functional homolog of yeast GPI10 (Fig. 4E).

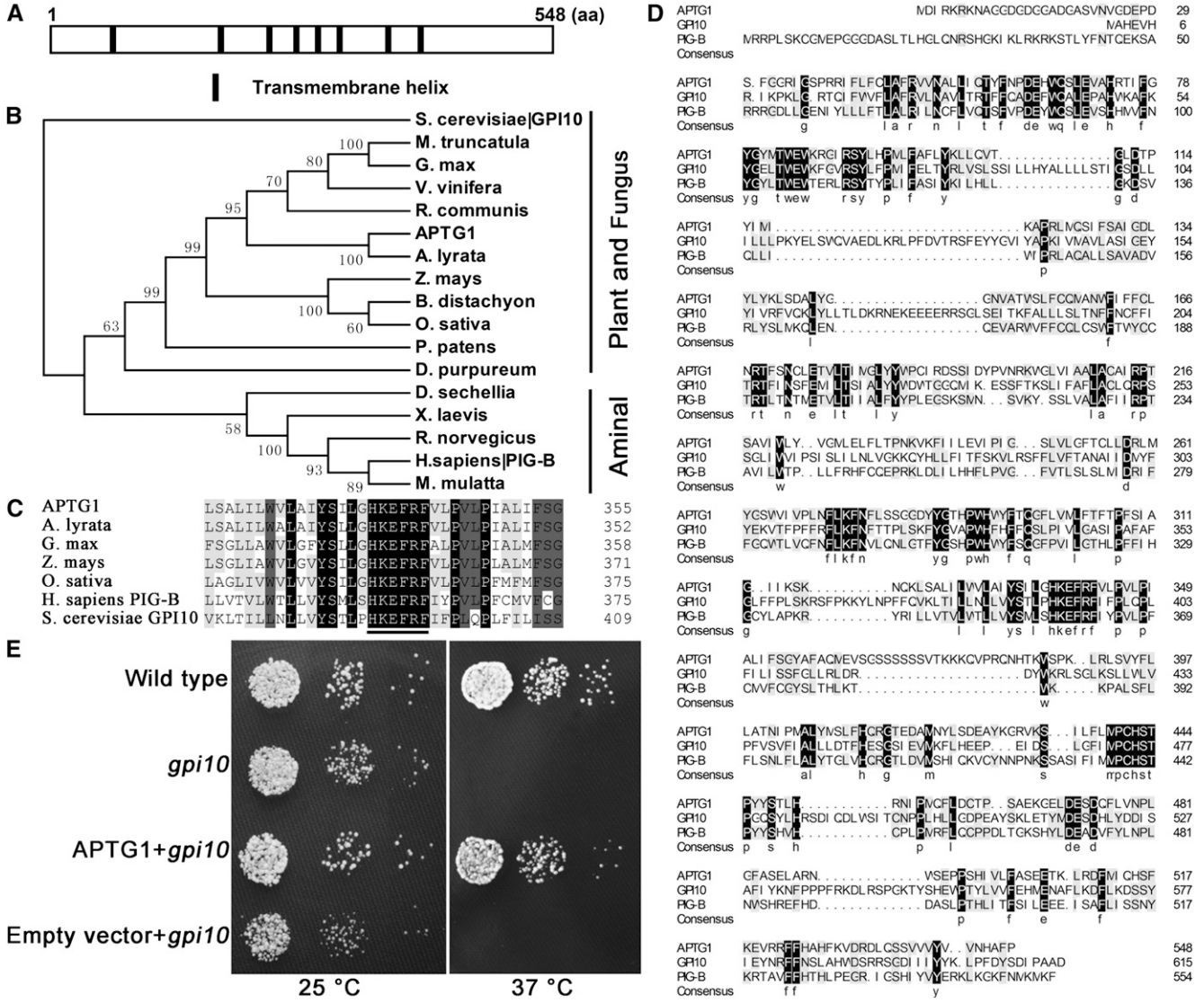

Figure 4. *APTG1* encoding a mannosyltransferase. A, Predicted transmembrane domains of APTG1. aa, Amino acids. B, Phylogenetic analysis of APTG1 (NP_568305.1) with its homologs in *A. lyrata* (XP_002873694.1), *Brachypodium distachyon* (XP_003571962.1), *Dictyostelium purpureum* (XP_003285528.1), *Drosophila sechellia* (XP_002035230.1), *G. max* (XP_003542300.1), human (AAH17711.1; PIG-B), *Macaca mulatta* (XP_002804830.1), *M. truncatula* (XP_003610240.1), *Oryza sativa* (NP_001043404.1, Os01g0580100), *Physcomitrella patens* (XP_001758335.1), *Rattus norvegicus* (EDL84114.1), *R. communis* (XP_002513232.1), yeast (DAA07968.1; GPI10), *V. vinifera* (XP_002271446.1), *Xenopus laevis* (NP_001089512.1), and *Zea mays* (ACL54567.1). C, Alignments of APTG1 and its homologs in *A. lyrata* (XP_002873694.1), *G. max* (XP_003542300.1), *Z. mays* (ACL54567.1), human (AAH17711.1; PIG-B), and yeast (DAA07968.1; GPI10) showing their conserved motif, HKEXRF (underlined). D, Full-length protein sequence alignment between APTG1, PIG-B in human (AAH17711.1), and GPI10 in yeast (DAA07968.1). Identical amino acids are labeled in black. E, APTG1 complements the thermosensitivity of the yeast mutant *gpi10*. The yeast YGL142c thermosensitivity strain (*gpi10* mutant) and the wild-type strain BY4741 could grow at 25°C. But the yeast YGL142c thermosensitivity strain could not grow at 37°C, although the BY4741 strain could. Compared with transformation with the empty vector pYES2, the yeast YGL142c TS strain transformed with pYES2 harboring *APTG1* complementary DNA could grow at 37°C.

APTG1 Is Localized at the ER

The expression of *APTG1* in various organs was determined by quantitative real-time (qRT)-PCR. *APTG1* showed higher expression in leaves, roots, stems, flowers, siliques, and pollen than in seedlings (Fig. 5A). To examine the expression patterns in detail, we detected both GUS and GFP signals in transgenic Arabidopsis harboring Pro_{APTG1}::*GUS* and Pro_{APTG1}::*APTG1-GFP*, respectively. *APTG1* was expressed in vascular tissue of seedlings, leaves, root tips, inflorescence stems, and flowers (Fig. 5, B–E). In pistils, *APTG1* expression was

detected in the ovary walls, styles, mature embryo sacs, and developing embryos (Fig. 5, F–I). In mature pollen grains at anthesis and in germinated pollen tubes, *APTG1* was much more highly expressed than in young pollen grains (Fig. 5, J–M). Because both PIG-B and GPI10 are ER membrane proteins (Maeda and Kinoshita, 2011), we tried to confirm whether APTG1 was an ER localization protein. The 35S::*APTG1-GFP* construct was introduced into Arabidopsis plants expressing the ER marker ER-rb (Nelson et al., 2007) by *A. tumefaciens*-mediated infiltration and examined by confocal microscopy. We found that APTG1 showed ER localization (Fig. 6A). Furthermore, to test whether APTG1 was localized in pollen tubes, we made a Pro_{APTG1}::*APTG1-GFP* construct, which was then transformed into the *aptg1/+* mutant. Indeed, Pro_{APTG1}::*APTG1-GFP* significantly

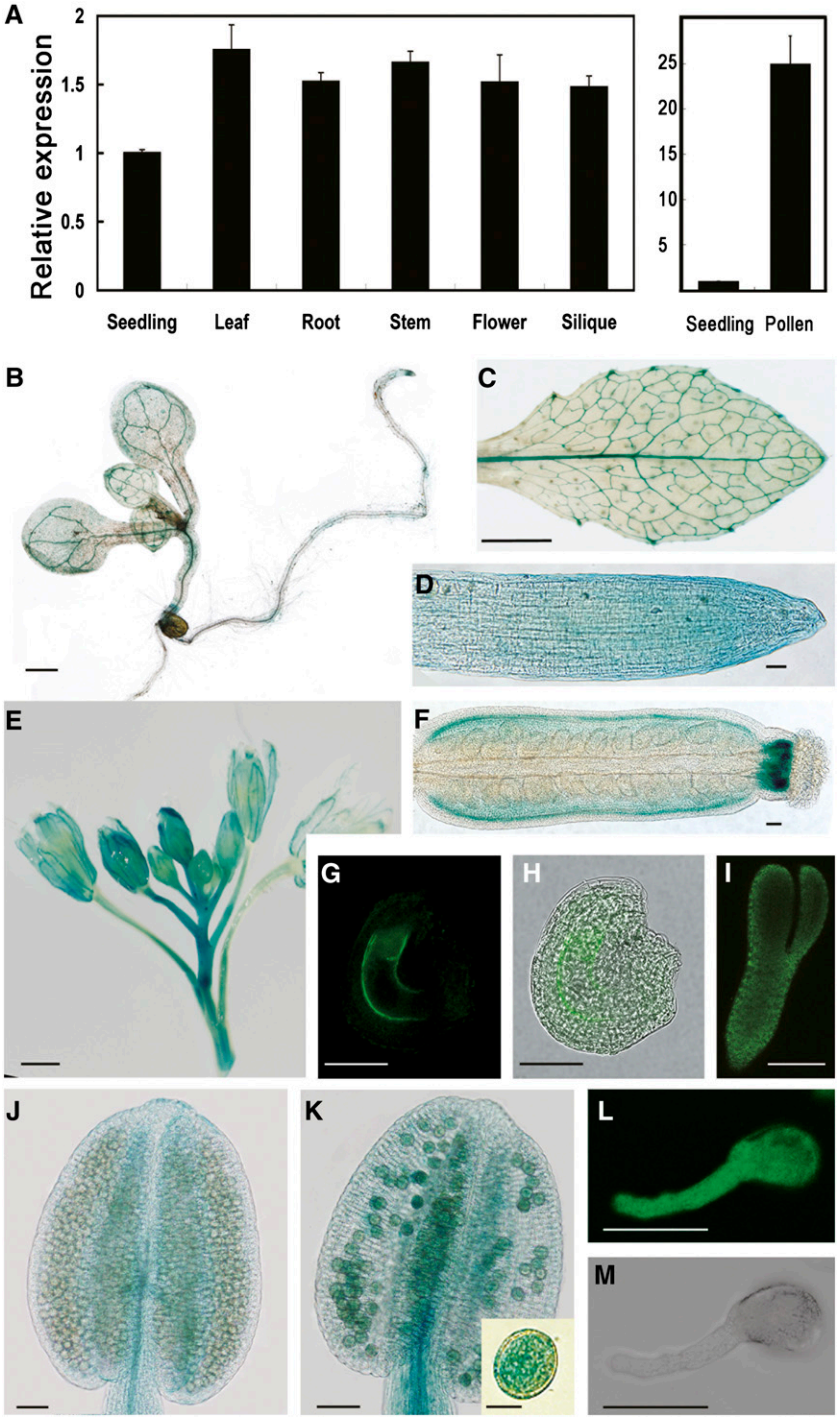

Figure 5. Expression pattern of *APTG1*. A, qRT-PCR analysis of *APTG1* expression in seedlings, leaves, roots, stems, flowers, siliques, and mature pollen grains. B to F, J, and K, GUS staining analysis in transgenic plants of Pro_{APTG1}::*GUS* showing the expression of *APTG1* in the seedling (B), leaf (C), root tip (D), inflorescence (E), pistil (F), immature pollen (J), and mature pollen (K). The inset in K is a magnified mature pollen grain. G, H, I, L, and M, GFP fluorescence analysis in transgenic plants of Pro_{APTG1}::*APTG1-GFP* showing the expression of *APTG1* in the embryo sac (G), torpedo embryo (I), and pollen tube (L). H and M are bright-field images of G and L, respectively. Bars = 10 μm (K inset), 50 μm (D, G, H, J–L, and M), 100 μm (F and I), 1 mm (B and E), and 5 mm (C).

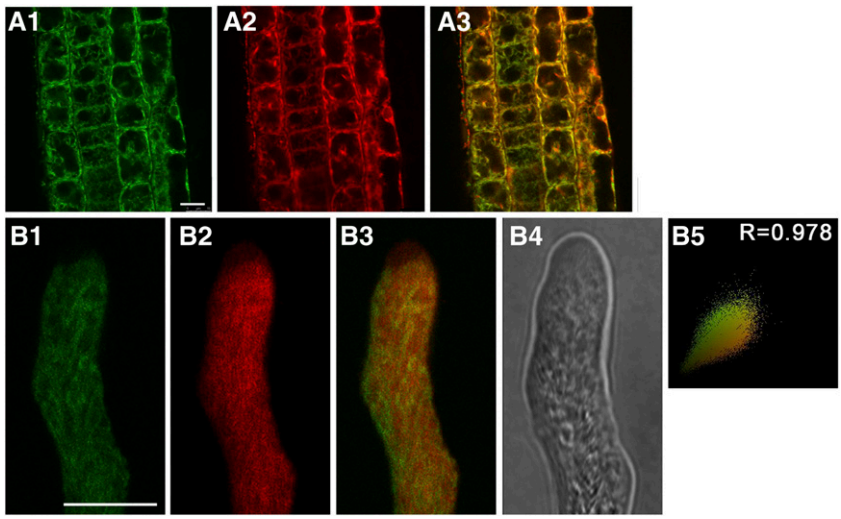

Figure 6. Subcellular localization of APTG1. A, Colocalization analysis of APTG1 and ER in the Arabidopsis meristem zone of root expressing *35S::APTG1-GFP* and the ER marker ER-rb. A1, A2, and A3 show APTG1-GFP, ER-rb, and merged images, respectively. B, Colocalization analysis of APTG1-GFP and ER in Arabidopsis pollen tubes expressing Pro_{APTG1}::*APTG1-GFP* stained with ER-Tracker Red. B1, B2, B3, and B4 show APTG1-GFP, ER-Tracker Red, merged, and bright-field images, respectively. B5 shows the Pearson correlation coefficient (R) analysis. Bars = 10 μm.

increased the transmission of the mutant *aptg1* allele by introducing Pro_{APTG1}::*APTG1-GFP* into the *aptg1*/+ mutant, suggesting the APTG1-GFP is functional in plants (Supplemental Table S1). The APTG1-GFP signal was also colocalized with the ER marker in a growing pollen tube expressing Pro_{APTG1}::*APTG1-GFP* (Fig. 6B), suggesting that APTG1 is an ER-localized protein in the pollen tube.

Functional Loss of *APTG1* Impairs the Apical PM Localization of COBL10 in Pollen Tubes

Our previous study showed that Arabidopsis COBL10, a GPI-AP, was important for the growth of pollen tubes in the transmitting tract of pistil (Li et al., 2013). The *cobl10* pollen tubes showed the compromised guidance growth toward micropyles similar to that in the *aptg1* mutant. COBL10 is a GPI-AP localized in the apical PM and cytoplasm in growing pollen tubes (Supplemental Fig. S7), and its PM localization depends on the GPI anchor (Li et al., 2013). We wondered whether the PM localization of COBL10 was altered in the *aptg1* mutant, because *APTG1* encodes a mannosyltransferase functioning in GPI anchor biosynthesis. Thus, we observed the localization of COBL10-citrine in the pollen tubes of the *aptg1*/+ mutant by introducing Pro_{COBL10}:*SP-citrine-COBL10* into the *aptg1*/+ mutant (Li et al., 2013). About 54.8% of *aptg1*/+ pollen tubes (n = 453) showed normal COBL10-citrine localization in the apical PM and the cytoplasm (Fig. 7, A and C), which is similar to that observed in the wild-type pollen tubes (Li et al., 2013). In contrast, some tubes (45.2%; n = 453) lost the apical PM localization of COBL10-citrine (Fig. 7, B and C). In the control, only one pollen tube (1.1%; n = 92) showed abnormal COBL10 localization in the 92 observed pollen tubes from the wild-type plants with Pro_{COBL10}:*SP-citrine-COBL10* (Fig. 7C). The fluorescence intensity of COBL10-citrine was very low in the apical region cytoplasm in the normal COBL10 localization of the pollen tube (Fig. 7, A and D), but the intensity was higher in the apical cytoplasm in the abnormal tube (Fig. 7, B and D). Additionally, the fluorescence intensity of COBL10-citrine in the cytoplasm of the subapical and shank regions of the *aptg1* mutant pollen tube did not show any difference from that of wild-type pollen tubes (Fig. 7D). A previous study showed that the Arabidopsis receptor-like kinases LIP1 and LIP2 are PM localized in growing pollen tubes and function in guiding pollen tube growth to the micropyle (Liu et al., 2013). Because these two LIPs are not GPI-APs, we used them as the control by investigating whether their localization was also changed in *aptg1* mutant pollen tubes. We found that the PM localization of LIP2-mRFP (for monomeric red fluorescent protein) did not show any changes in the *aptg1*/+ mutant pollen tubes expressing Pro_{LIP2}::*LIP2-mRFP* compared with the wild-type tubes expressing Pro_{LIP2}::*LIP2-mRFP* (Supplemental Fig. S8). These results suggest that the *aptg1* mutation disrupts the localization of GPI-APs in the PM of the pollen tube.

DISCUSSION

Processing of GPI anchors mainly occurs in the ER, and at least 16 PIG proteins participate in this process (Maeda and Kinoshita, 2011). PIG-B in human functions in GPI anchor biosynthesis by adding the third Man to the backbone of GPI anchors (Takahashi et al., 1996). GPI10 is a yeast homolog of PIG-B. Mutation of GPI10 led to cell death in yeast (Sütterlin et al., 1998). In this study, we showed that APTG1 is a functional homolog of PIG-B and GPI10 and is localized in the ER. The *aptg1* mutant is defective in pollen tube guidance and embryo development, suggesting that APTG1 functions in GPI anchor biosynthesis. Previous studies demonstrated that defects in GPI anchor biosynthesis led

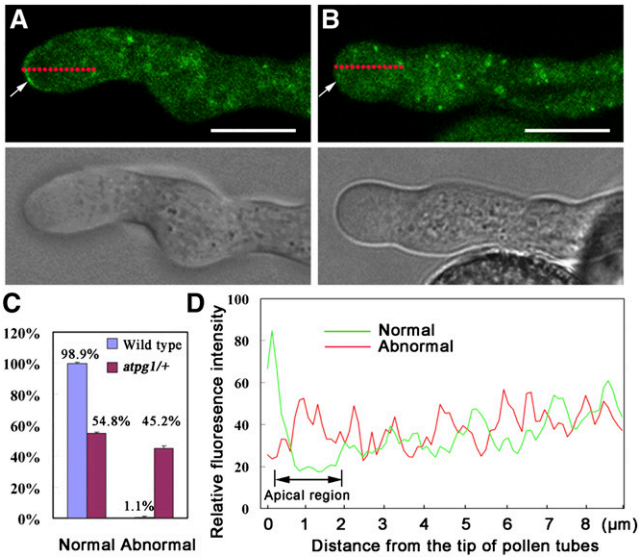

Figure 7. Localization of citrine-COBL10 in pollen tubes of the *aptg1*/+ mutant. A, Citrine-COBL10 showing normal PM localization (arrow) in the tip of the *aptg1/+* pollen tube expressing Pro_{COBL10}*:SP-citrine-COBL10*. B, Citrine-COBL10 showing abnormal PM localization (arrow) in the tip of the *aptg1/+* pollen tube expressing Pro_{COBL10}*:SP-citrine-COBL10*. C, Percentage of pollen tubes showing normal and abnormal PM localization of citrine-COBL10 (n = 453) in the wild type and the *aptg1/+* mutant. D, Relative fluorescence intensity through the red lines in the tips of pollen tubes showing normal (A) and abnormal (B) PM localization expressing citrine-COBL 10 in *aptg1/+*. Bars = 10 μm.

to abnormal reproductive development in Arabidopsis. For example, Arabidopsis *SETH1* and *SETH2* encode homologs of PIG-C and PIG-A, respectively. The disruption of *SETH1* and *SETH2* in Arabidopsis resulted in reduced pollen germination and tube growth by interfering with pollen tube wall deposition or metabolism (Lalanne et al., 2004). Arabidopsis *PEANUT1*, encoding a putative PIG-M, is important for pollen viability and embryo development (Gillmor et al., 2005). Additionally, we found that *APTG1* plays a role in seedling growth by using an RNA interference approach. These studies indicate that deficiency in GPI biosynthesis leads to defects in the vegetative and reproductive development of plants. Identification of the GPI-APs whose processing and targeting are disturbed in the Arabidopsis PIG-defect mutants would give a deeper insight into the biological roles of GPI anchors and GPI-APs in plant vegetative and reproductive development.

Deficiency in GPI biosynthesis interferes with the correct targeting of GPI-APs to the PM (Fujita and Kinoshita, 2012). However, few GPI-APs have been reported in plants. COBL10 is a GPI-AP localized in the apical PM of growing pollen tubes, and pollen tubes of the *cobl10* mutants showed compromised ovule guidance (Li et al., 2013). In pollen tubes of the *aptg1* mutant, the apical PM localization of COBL10 was lost. COBL10 also lost its apical membrane localization in the *seth1* and *seth2* mutants (Li et al., 2013). We suggest that the defect of GPI anchor biosynthesis caused the mistargeting of COBL10. At least 47 genes expressed in pollen potentially encode GPI-APs, and at least 11 of these proteins are associated with pollen membranes by GPI anchoring (Lalanne et al., 2004). There are a number of Arabidopsis genes encoding predicted GPI-APs with enhanced expression in germinating pollen tubes in vitro or in tubes growing through the stigma and style, such as lipid-transfer protein genes and arabinogalactan protein genes (Wang et al., 2008; Qin et al., 2009). These predicted GPI-APs might be important for pollen tube growth and micropylar guidance; however, whether they are targeted to the PM and whether their localizations are altered in *aptg1* mutant pollen tubes remain to be investigated. Additionally, *aptg1* showed embryo lethality, which is different from *cobl10* (Li et al., 2013). It is possible that the localizations of other substrates of APTG1, functioning in embryo development, were lost in *aptg1*. Several studies suggested that receptors localized at the apical PM of pollen tubes were candidates for perceiving attractive signals from female tissues (Tang et al., 2002, 2004; Chae and Lord, 2011; Michard et al., 2011; Liu et al., 2013). The addition of a GPI anchor provides an alternative strategy for the external localization of receptor proteins on the PM (Fujita and Kinoshita, 2012). Some GPI-anchored receptors were identified in the PM of mammalian cells, such as folate receptor and urokinase-type plasminogen activator receptor (Kinoshita et al., 2008). In *aptg1* pollen tubes, some GPI-anchored receptors involved in sensing the signal molecules from the female tissues might lose their membrane localization, which led to the misguidance of *aptg1* pollen tubes. The identification of such GPI-anchored receptors in pollen tubes will help us understand the mechanism of pollen tube guidance by female tissues.

cobl10 pollen tubes grew slowly in the transmitting tract, which resulted from changes in the wall structure and the distribution of esterified pectins in the pollen tube (Li et al., 2013). However, the pollen tube growth of *aptg1* did not show obvious abnormality, and the distribution of both esterified and deesterified pectins in pollen tubes of the *aptg1* mutant was not altered (Supplemental Fig. S9). In SP-citrine-COBL10ΔC9, the last nine amino acids of COBL10 proteins were replaced by an Asn residue (Li et al., 2013), which may impair its biochemical function in cell wall formation due to mislocalization. In *aptg1*, COBL10 lost its localization at the apical PM of pollen tubes. Previous studies suggested that GPI-APs could be released from the membrane after cleavage by specific phospholipases and become free proteins that potentially serve as signals, diffusible enzymes, or structural components (Roudier et al., 2002). COBL10 was localized at the apical PM and in the cytoplasm of pollen tubes (Li et al., 2013). Here, we showed that the localization of COBL10 in the cytoplasm of the subapical and shank regions was not changed in the *aptg1* pollen tubes compared with that of the wild type, and more COBL10 protein

was localized in the apical cytoplasm in the *aptg1* mutant (Fig. 7D). COBL10 localized in the cytoplasm of the *aptg1* pollen tubes may still function in cell wall construction and pollen tube growth. The different COBL10 distributions between the *cobl10* and *aptg1* mutants might result in the difference of pollen tube phenotypes in these mutants.

Most PIG proteins involved in GPI biosynthesis are localized in the ER (Maeda and Kinoshita, 2011). In this study, we demonstrated that APTG1 is also an ER-localized protein. Immunoblot analysis showed that APTG1 is only detected in the microsomal fraction, indicating that APTG1 is an integral membrane protein (Supplemental Fig. S10). Thus, the localization of APTG1 is similar to that of yeast GPI10. To date, several male factors that are endomembrane localized have been shown to be involved in the perception of female cues during pollen tube growth. For example, the Arabidopsis sperm cell-specific protein HAPLESS2/GENERATIVE CELL-SPECIFIC1, which is involved in pollen tube micropylar targeting, is mainly localized in the ER membrane (von Besser et al., 2006), whereas the Arabidopsis Rab GTPase RABA4D is localized in an endomembrane at the tips of growing pollen tubes (Szumlanski and Nielsen, 2009). The Arabidopsis K^+ transporters CHX21 and CHX23 are localized at the ER membrane in growing pollen tubes (Lu et al., 2011). POD1 is an ER luminal protein involved in ER protein retention and folding by interacting with ER-resident factors in growing pollen tubes (Li et al., 2011). These studies indicate the importance of the endomembrane system, especially the ER, in directing pollen tube growth. Posttranslational modifications and protein quality control occurring in the ER are required for receptor targeting as well as receptor maturation during cell signaling in plants (Li and Yang, 2012). We propose that signal proteins involved in pollen tube guidance require modifications occurring in the ER for maturation and functionality. Further studies on the ER functions are required for understanding the mechanism of pollen tube guidance.

MATERIALS AND METHODS

Plant Materials and Growth Conditions

Arabidopsis (*Arabidopsis thaliana*) SALK_080854 seeds were obtained from The Arabidopsis Information Resource seed stock center. The genotypes of SALK_080854 mutant plants were determined by a PCR-based method (primers LBb1.3, LP1, and RP1). Seeds of the mutant and transgenic lines were plated onto medium supplemented with 50 mg L^{-1} kanamycin for SALK_080854 and with 30 mg L^{-1} hygromycin for transgenic lines harboring pCAMBIA-based constructs. Wild-type (Columbia-0) and mutant Arabidopsis plants were grown as reported previously by Xu et al. (2011). All primer sequences are listed in Supplemental Table S2.

Analysis of Pollen Grains, Pollen Tubes, and Embryos

Alexander staining for pollen viability analysis and DAPI staining for nuclei were performed as described by Alexander (1969) and Ross et al. (1996), respectively. For the pollen in vitro germination assay, mature pollen grains were spread onto pollen germination medium (pH 7) containing 1 mM $CaCl_2$, 1 mM $Ca(NO_3)_2$, 1 mM $MgSO_4$, 0.01% (w/v) H_3BO_4, 18% (w/v) Suc, and 0.8% (w/v) agarose, then the pollen tubes were observed after 3 to 6 h at 28°C. Aniline Blue staining for pollen tube growth in vivo was performed as described by Chen et al. (2007). For the observation of embryo development, the pistils (3–4 d after limited pollination) were incubated in Hoyer's solution (chloralhydrate:distilled water:glycerol = 8:3:1) for 45 min at 4°C, then cleared at room temperature for 24 h, and viewed with differential interference contrast, as described by Gillmor et al. (2005). All images were photographed with a BX51 microscope (Olympus).

qRT-PCR Analysis of *APTG1* Expression

Seedlings (3 weeks old) and roots, stems, leaves, flowers, and siliques from 5-week-old plants were collected for total RNA isolation using the Trizol isolation reagent (Invitrogen), and mature pollen total RNA was isolated with the RNeasy Plant Mini Kit (catalog no. 74904; Qiagen). qRT-PCR analysis was conducted using the primer pair *APTG1*RT-sense and *APTG1*RT-antisense. Tubulin was used as a quantitative control and amplified using the primer pair TUB2-sense and TUB2-antisense. All experiments involved three biological repeats. All primer sequences are listed in Supplemental Table S2.

Plasmid Construction and Plant Transformation

For the complementation construct, a 3,434-bp fragment containing a 1,799-bp predicted promoter sequence (amplified with primers *pAPTG1-S2* and *pAPTG1-A2* from Arabidopsis genomic DNA) and the CDS (amplified with primers *APTG1GFP-S* and *APTG1-A* from Arabidopsis floral complementary DNA) were ligated to pCAMBIA1300. This construct was transformed into *aptg1*/+ mutant plants. To analyze the expression pattern of *APTG1*, the 1,799-bp promoter region amplified with primer pair *pAPTG1-S* and *pAPTG1-A* was inserted into pCAMBIA1391-GUS to generate Pro_{APTG1}::*GUS*. For the subcellular localization analysis of APTG1, Pro_{APTG1}::*APTG1-GFP* was made by subcloning the promoter and CDS of *APTG1* into *pCMBIA1300-eGFP*, in which the promoter sequence was amplified with primer pair *pAPTG1-S2* and *pAPTG1-A2*, and the CDS amplified with primer pair *APTG1GFP-S* and *APTG1GFP-A* was inserted above the GFP sequence. For the construct 35S::*APTG1-GFP*, the full-length genomic fragment of *APTG1* amplified with primers *APTG1-GFP-S* and *APTG1-GFP-A* was cloned into *pMDC83* using Gateway technology (Invitrogen). The amiRNA targeting *APTG1* was constructed as described previously. Primers (Ami-A, Ami-B, Ami-I, Ami-II, Ami-III, and Ami-IV) designed using WMD3 Web microRNA Designer (http://wmd3.weigelworld.org/cgi-bin/webapp.cgi) were used to amplify the amiRNA precursor by overlapping PCR from the pRS300 template. The fragment containing the amiRNA foldback was cloned into pJET 1.2/blunt cloning vector (Fermentas; K1231), sequenced, and subsequently cloned into the PROKII vector under the control of the cauliflower mosaic virus 35S and Lat52 promoters, forming 35S::*amiRNA-APTG1* and Lat52::*amiRNA-APTG1* for whole plants and pollen-specific expression, respectively. These constructs were transformed into wild-type plants. All primer sequences are listed in Supplemental Table S2.

SEM

To observe the pollen morphology, dry mature pollen grains coated with gold palladium were observed with a JSM-6610LV scanning electron microscope (JEOL) and photographed. To observe pollen tube growth in pistils, pollinated pistils were fixed with 3% (v/v) glutaraldehyde in 50 mM cacodylate buffer (pH 7). After an initial fixation at room temperature under a gentle vacuum, pistils were kept in fresh fixative at 4°C overnight. The specimens were then washed five times in phosphate buffer solution and postfixed in 1% (w/v) osmic acid (Sigma-Aldrich) for 5 h at 4°C. The fixed pistils were rinsed five times in phosphate-buffered saline buffer, dehydrated in a graded ethanol series, and critical point dried in liquid carbon dioxide. Finally, the dry pistils were observed with the scanning electron microscope and photographed.

Confocal Microscopy

The pollen tubes and pistils from transgenic plants expressing Pro_{APTG1}::*APTG1-GFP* were used for the expression pattern analysis of *APTG1*. For the subcellular localization of APTG1, the 35S::APTG1-GFP construct was introduced into Arabidopsis plants expressing ER-rb. The pollen tubes expressing Pro_{APTG1}::*APTG1-GFP* stained with ER-Tracker Red (Invitrogen; catalog no. E34250) were used for further analysis of the subcellular localization of APTG1

in pollen tubes. For the localization analysis of COBL10 and LIP2 in the *aptg1/+* mutant, we used pollen tubes expressing Pro_{COBL10}::*SP-citrine-COBL10* in *cobl10* and Pro_{LIP2}::*LIP2-mRFP* in the *aptg1/+* mutant background, respectively. APTG1-GFP was excited at 488 nm, and emissions were collected at 505 to 530 nm. ER-rb and ER-Tracker Red were excited using a 561-nm laser, and the emissions were observed at 600 to 630 nm. COBL10-citrine and LIP2-mRFP were excited at 514 and 561 nm, and the emissions were collected at 525 to 600 nm and 570 to 660 nm, respectively. Immunofluorescence labeling was performed with JIM5 and JIM7 as described (Li et al., 2013). Images were captured with a TCS SP5II confocal laser scanning microscope (Leica).

GUS Assays

GUS staining was performed according to Sieburth and Meyerowitz (1997). Flowers, siliques, and seedlings were incubated in GUS staining solution [1 mg mL^{-1} 5-bromo-4-chloro-3-indolyl-β-glucuronic acid (Biosynth), 2 mM $K_4Fe(CN)_6$, 2 mM $K_3Fe(CN)_6$, and 0.1% [v/v] Triton X-100 in 50 mM sodium phosphate buffer, pH 7] for 2 to 3 d at 37°C. The stained samples were cleared in 70% (v/v) ethanol. Stained specimens were visualized and photographed with an Olympus BX51 microscope equipped with a CCD camera.

Complementation of the Yeast *gpi10* Mutant

For complementation of the yeast (*Saccharomyces cerevisiae*) *gpi10* mutant, the CDS region of *APTG1* was amplified with primers APTG1HBy-S and APTG1HBy-A and ligated to pYES2. The genotype for the wild-type strain BY4741 is MATa his3Δ1 leu2Δ0 met15Δ0 ura3Δ0. The *gpi10* deletion mutant YGL142c thermosensitive strain was derived from the yeast magic marker heterozygous gene deletion collection (MATa/α ura3Δ0/ura3Δ0 leu2Δ0/leu2Δ0 his3Δ1/his3Δ1 lys2Δ0/LYS2 met15Δ0/MET15 can1Δ::LEU2-MFA1pr::His-3/CAN1 yfgΔ::KanMX/YFG). The haploid YGL142c thermosensitive strain had the following genotype: MATa ura3Δ0 leu2Δ0 his3Δ1 lys2Δ0 (or LYS2) met15Δ0 (or MET15) can1Δ::LEU2-MFA1pr::His-3 yfeg-ts::URA3. The selective plate contained 20 g L^{-1} Gal, 10 g L^{-1} yeast extract, and 20 g L^{-1} peptone. All primer sequences are listed in Supplemental Table S2.

Sequence data from this article can be found in the GenBank/EMBL data libraries under accession numbers NP_568305.1 (APTG1), AAH17711.1 (PIG-B), and DAA07968.1 (GPI10).

Supplemental Data

The following materials are available in the online version of this article.

Supplemental Figure S1. The plants and number of seeds of the wild type and *aptg1/+* mutant.

Supplemental Figure S2. Growth of pollen tubes of the wild type and *aptg1/+* in the style and transmitting tract of the wild type.

Supplemental Figure S3. Analysis of *aptg1/+* pollen tube guidance by scanning electron microscopy.

Supplemental Figure S4. Micropylar guidance of pollen tubes of a complementary transgenic line of *aptg1/+* $APTG1_{CDS}$.

Supplemental Figure S5. Micropylar guidance of pollen tubes of transgenic lines expressing *Lat52*::*amiRNA-APTG1*.

Supplemental Figure S6. The T3 seedling of 35S::amiRNA-*APTG1* transgenic lines.

Supplemental Figure S7. The COBL10 subcellular localization observed in the wild type pollen tube.

Supplemental Figure S8. The plasma membrane-localization of LIP2 in the wild type and *aptg1/+* mutant pollen tubes.

Supplemental Figure S9. Immunofluorescence labelling of pectins in semi-in vivo pollen tubes.

Supplemental Figure S10. Immunoblot analysis for the localization of APTG1.

Supplemental Table S1. Segregation analysis of the selfed progenies of *aptg1/+* mutant and *aptg1/+* $APTG1_{CDS}$-*GFP* lines.

Supplemental Table S2. Sequences of the primers.

ACKNOWLEDGMENTS

We thank all persons who provided materials for this study. The origins of the materials were as follows: Pro_{COBL10}:*SP-citrine-COBL10* transgenic plants (Dr. Yan Zhang, Shandong Agricultural University); Pro_{LIP2}::*LIP2-mRFP* seeds (Dr. Li-Jia Qu, Peking University); ER-rb seeds (Dr. Lei Ge, Shandong Agricultural University); yeast BY4741 and YGL142c thermosensitive strains (Dr. Junbiao Dai, Tsinghua University); antibodies against PDIL1 and CNX1 (Dr. Qi Xie, Chinese Academy of Sciences); pRS300 vector (Dr. Detlef Weigel, Max Planck Institute for Developmental Biology); and T-DNA insertion line SALK_080854 (Arabidopsis Biological Resource Center).

Received January 17, 2014; accepted June 23, 2014; published June 24, 2014.

LITERATURE CITED

Alandete-Saez M, Ron M, McCormick S (2008) GEX3, expressed in the male gametophyte and in the egg cell of *Arabidopsis thaliana*, is essential for micropylar pollen tube guidance and plays a role during early embryogenesis. Mol Plant **1:** 586–598

Alexander MP (1969) Differential staining of aborted and nonaborted pollen. Stain Technol **44:** 117–122

Capron A, Gourgues M, Neiva LS, Faure JE, Berger F, Pagnussat G, Krishnan A, Alvarez-Mejia C, Vielle-Calzada JP, Lee YR, et al (2008) Maternal control of male-gamete delivery in *Arabidopsis* involves a putative GPI-anchored protein encoded by the *LORELEI* gene. Plant Cell **20:** 3038–3049

Chae K, Lord EM (2011) Pollen tube growth and guidance: roles of small, secreted proteins. Ann Bot (Lond) **108:** 627–636

Chen YH, Li HJ, Shi DQ, Yuan L, Liu J, Sreenivasan R, Baskar R, Grossniklaus U, Yang WC (2007) The central cell plays a critical role in pollen tube guidance in *Arabidopsis*. Plant Cell **19:** 3563–3577

Ching A, Dhugga KS, Appenzeller L, Meeley R, Bourett TM, Howard RJ, Rafalski A (2006) Brittle stalk 2 encodes a putative glycosylphosphatidylinositol-anchored protein that affects mechanical strength of maize tissues by altering the composition and structure of secondary cell walls. Planta **224:** 1174–1184

DeBono A, Yeats TH, Rose JK, Bird D, Jetter R, Kunst L, Samuels L (2009) *Arabidopsis* LTPG is a glycosylphosphatidylinositol-anchored lipid transfer protein required for export of lipids to the plant surface. Plant Cell **21:** 1230–1238

Dresselhaus T, Franklin-Tong N (2013) Male-female crosstalk during pollen germination, tube growth and guidance, and double fertilization. Mol Plant **6:** 1018–1036

Fujita M, Kinoshita T (2012) GPI-anchor remodeling: potential functions of GPI-anchors in intracellular trafficking and membrane dynamics. Biochim Biophys Acta **1821:** 1050–1058

Gillmor CS, Lukowitz W, Brininstool G, Sedbrook JC, Hamann T, Poindexter P, Somerville C (2005) Glycosylphosphatidylinositol-anchored proteins are required for cell wall synthesis and morphogenesis in *Arabidopsis*. Plant Cell **17:** 1128–1140

Higashiyama T, Kuroiwa H, Kuroiwa T (2003) Pollen-tube guidance: beacons from the female gametophyte. Curr Opin Plant Biol **6:** 36–41

Howden R, Park SK, Moore JM, Orme J, Grossniklaus U, Twell D (1998) Selection of T-DNA-tagged male and female gametophytic mutants by segregation distortion in *Arabidopsis*. Genetics **149:** 621–631

Jones-Rhoades MW, Borevitz JO, Preuss D (2007) Genome-wide expression profiling of the *Arabidopsis* female gametophyte identifies families of small, secreted proteins. PLoS Genet **3:** 1848–1861

Kasahara RD, Portereiko MF, Sandaklie-Nikolova L, Rabiger DS, Drews GN (2005) MYB98 is required for pollen tube guidance and synergid cell differentiation in *Arabidopsis*. Plant Cell **17:** 2981–2992

Kessler SA, Grossniklaus U (2011) She's the boss: signaling in pollen tube reception. Curr Opin Plant Biol **14:** 622–627

Kinoshita T, Fujita M, Maeda Y (2008) Biosynthesis, remodelling and functions of mammalian GPI-anchored proteins: recent progress. J Biochem **144:** 287–294

Lalanne E, Honys D, Johnson A, Borner GH, Lilley KS, Dupree P, Grossniklaus U, Twell D (2004) *SETH1* and *SETH2*, two components of the glycosylphosphatidylinositol anchor biosynthetic pathway, are required for pollen germination and tube growth in *Arabidopsis*. Plant Cell **16:** 229–240

Li HJ, Xue Y, Jia DJ, Wang T, Hi DQ, Liu J, Cui F, Xie Q, Ye D, Yang WC (2011) POD1 regulates pollen tube guidance in response to micropylar

female signaling and acts in early embryo patterning in *Arabidopsis*. Plant Cell **23:** 3288–3302

Li HJ, Yang WC (2012) Emerging role of ER quality control in plant cell signal perception. Protein Cell **3:** 10–16

Li S, Ge FR, Xu M, Zhao XY, Huang GQ, Zhou LZ, Wang JG, Kombrink A, McCormick S, Zhang XS, et al (2013) *Arabidopsis* COBRA-LIKE 10, a GPI-anchored protein, mediates directional growth of pollen tubes. Plant J **74:** 486–497

Liu J, Zhong S, Guo X, Hao L, Wei X, Huang Q, Hou Y, Shi J, Wang C, Gu H, et al (2013) Membrane-bound RLCKs LIP1 and LIP2 are essential male factors controlling male-female attraction in *Arabidopsis*. Curr Biol **23:** 993–998

Lu Y, Chanroj S, Zulkifli L, Johnson MA, Uozumi N, Cheung A, Sze H (2011) Pollen tubes lacking a pair of K^+ transporters fail to target ovules in *Arabidopsis*. Plant Cell **23:** 81–93

Maeda Y, Kinoshita T (2011) Structural remodeling, trafficking and functions of glycosylphosphatidylinositol-anchored proteins. Prog Lipid Res **50:** 411–424

Márton ML, Cordts S, Broadhvest J, Dresselhaus T (2005) Micropylar pollen tube guidance by *egg apparatus 1* of maize. Science **307:** 573–576

Michard E, Lima PT, Borges F, Silva AC, Portes MT, Carvalho JE, Gilliham M, Liu LH, Obermeyer G, Feijó JA (2011) Glutamate receptor-like genes form Ca^{2+} channels in pollen tubes and are regulated by pistil D-serine. Science **332:** 434–437

Nelson BK, Cai X, Nebenführ A (2007) A multicolored set of in vivo organelle markers for co-localization studies in *Arabidopsis* and other plants. Plant J **51:** 1126–1136

Okuda S, Tsutsui H, Shiina K, Sprunck S, Takeuchi H, Yui R, Kasahara RD, Hamamura Y, Mizukami A, Susaki D, et al (2009) Defensin-like polypeptide LUREs are pollen tube attractants secreted from synergid cells. Nature **458:** 357–361

Oriol R, Martinez-Duncker I, Chantret I, Mollicone R, Codogno P (2002) Common origin and evolution of glycosyltransferases using Dol-P-monosaccharides as donor substrate. Mol Biol Evol **19:** 1451–1463

Qin Y, Leydon AR, Manziello A, Pandey R, Mount D, Denic S, Vasic B, Johnson MA, Palanivelu R (2009) Penetration of the stigma and style elicits a novel transcriptome in pollen tubes, pointing to genes critical for growth in a pistil. PLoS Genet **5:** e1000621

Ross KJ, Fransz P, Jones GH (1996) A light microscopic atlas of meiosis in *Arabidopsis thaliana*. Chromosome Res **4:** 507–516

Roudier F, Schindelman G, DeSalle R, Benfey PN (2002) The COBRA family of putative GPI-anchored proteins in Arabidopsis: a new fellowship in expansion. Plant Physiol **130:** 538–548

Schwab R, Ossowski S, Riester M, Warthmann N, Weigel D (2006) Highly specific gene silencing by artificial microRNAs in *Arabidopsis*. Plant Cell **18:** 1121–1133

Shimizu KK, Okada K (2000) Attractive and repulsive interactions between female and male gametophytes in *Arabidopsis* pollen tube guidance. Development **127:** 4511–4518

Sieburth LE, Meyerowitz EM (1997) Molecular dissection of the *AGAMOUS* control region shows that *cis* elements for spatial regulation are located intragenically. Plant Cell **9:** 355–365

Sütterlin C, Escribano MV, Gerold P, Maeda Y, Mazon MJ, Kinoshita T, Schwarz RT, Riezman H (1998) *Saccharomyces cerevisiae* GPI10, the functional homologue of human PIG-B, is required for glycosylphosphatidylinositol-anchor synthesis. Biochem J **332:** 153–159

Szumlanski AL, Nielsen E (2009) The Rab GTPase RabA4d regulates pollen tube tip growth in *Arabidopsis thaliana*. Plant Cell **21:** 526–544

Takahashi M, Inoue N, Ohishi K, Maeda Y, Nakamura N, Endo Y, Fujita T, Takeda J, Kinoshita T (1996) PIG-B, a membrane protein of the endoplasmic reticulum with a large lumenal domain, is involved in transferring the third mannose of the GPI anchor. EMBO J **15:** 4254–4261

Takeuchi H, Higashiyama T (2011) Attraction of tip-growing pollen tubes by the female gametophyte. Curr Opin Plant Biol **14:** 614–621

Tang W, Ezcurra I, Muschietti J, McCormick S (2002) A cysteine-rich extracellular protein, LAT52, interacts with the extracellular domain of the pollen receptor kinase LePRK2. Plant Cell **14:** 2277–2287

Tang W, Kelley D, Ezcurra I, Cotter R, McCormick S (2004) LeSTIG1, an extracellular binding partner for the pollen receptor kinases LePRK1 and LePRK2, promotes pollen tube growth in vitro. Plant J **39:** 343–353

Tsukamoto T, Qin Y, Huang Y, Dunatunga D, Palanivelu R (2010) A role for LORELEI, a putative glycosylphosphatidylinositol-anchored protein, in *Arabidopsis thaliana* double fertilization and early seed development. Plant J **62:** 571–588

von Besser K, Frank AC, Johnson MA, Preuss D (2006) *Arabidopsis HAP2* (*GCS1*) is a sperm-specific gene required for pollen tube guidance and fertilization. Development **133:** 4761–4769

Wang Y, Zhang WZ, Song LF, Zou JJ, Su Z, Wu WH (2008) Transcriptome analyses show changes in gene expression to accompany pollen germination and tube growth in Arabidopsis. Plant Physiol **148:** 1201–1211

Xu N, Gao XQ, Zhao XY, Zhu DZ, Zhou LZ, Zhang XS (2011) *Arabidopsis* AtVPS15 is essential for pollen development and germination through modulating phosphatidylinositol 3-phosphate formation. Plant Mol Biol **77:** 251–260